Figure S1

Figure S1. KDM5 gene-dependent patient overall survival across different cancer entities, Related to Figure 1. (**A**) Kaplan-Meier survival curves for KDM5B across different cancer entities. Curves were calculated from the TCGA data set based on a 10% gene expression threshold (10% highest expression, black, vs. 10% lowest, red). Graphs were created by the TCGA browser tool v0.9. (**B**) Kaplan-Meier survival curves of melanoma patients for KDM5A, KDM5C, and KDM5D. **(C)** Quantitated anti-KDM5B immunostaining shown as normalised frequency distribution of nuclear staining intensity. Treatment-naïve 451Lu melanoma cells were exposed to 10 µM PLX4720 over 72 h and compared to the DMSO control (left panel). Chronically resistant 451LuBR cells were maintained under the presence of 1 µM PLX4720 and compared to naïve 451Lu under DMSO treatment (right panel).
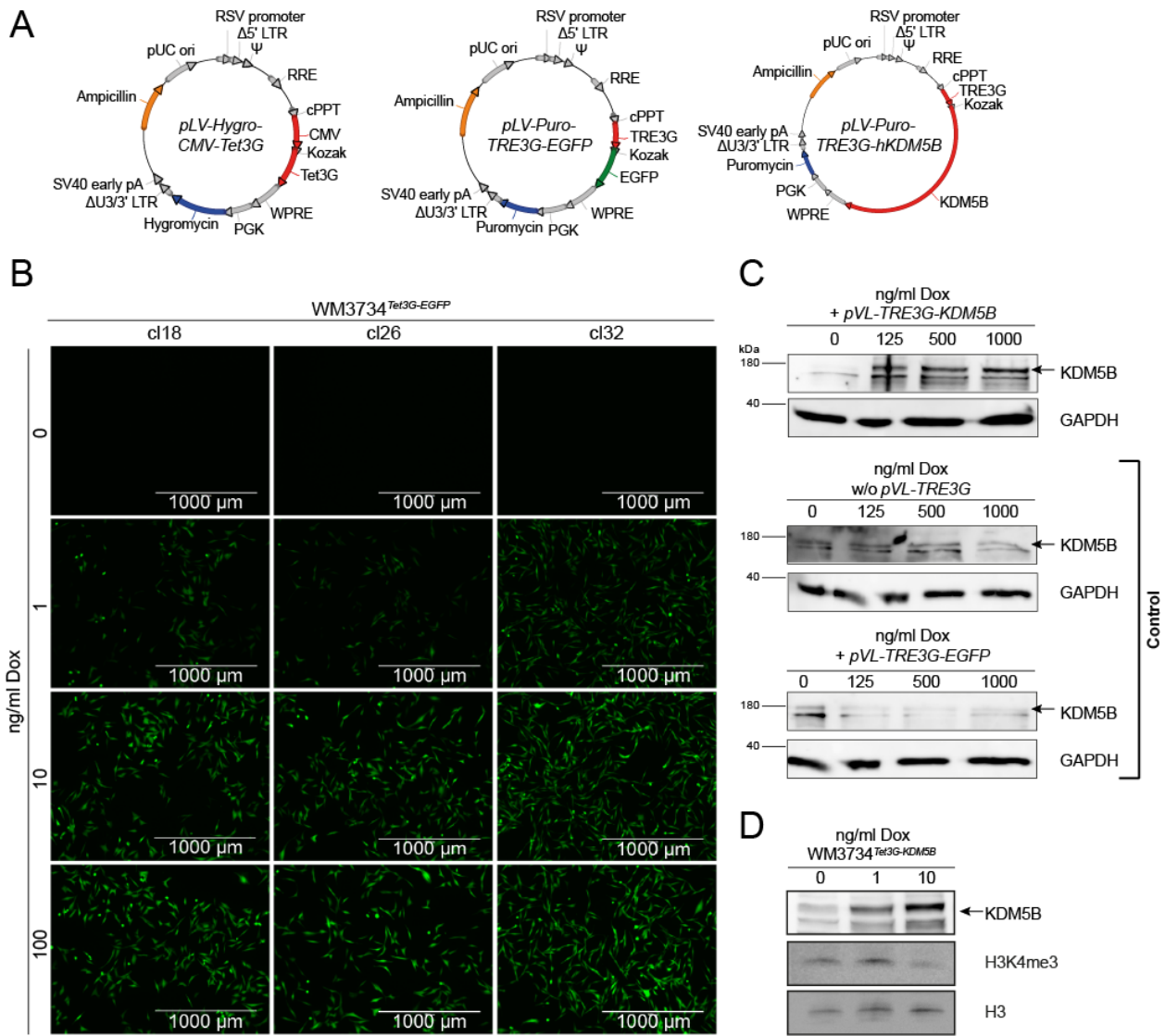
Figure S2

Figure S2. Establishment of a doxycycline-inducible Tet-On 3G-system for KDM5B protein overexpression, Related to Figure 1. (**A**) Vector maps of the plasmid encoding the CMV promoter-driven Tet3G (left, pLV-Hygro-CMV-Tet3G), the TRE response vector with an inducible P_{TRE3G} promoter plus the control gene EGFP (middle, pLV-Puro-TRE3G-EGFP), and the TRE response vector with an inducible P_{TRE3G} promoter plus the human KDM5B gene (right, pLV-Puro-

TRE3G-hKDM5B, transcript variant 1, NM_001314042.1). (**B**) EGFP protein induction at increasing Dox concentrations in three different clones of stably transduced WM3734[Tet3G-EGFP] control cells imaged after 48 h of induction. (**C**) Immunoblotting of KDM5B protein induction in WM3734[Tet3G] cells transduced with pVL-TRE3G-KDM5B at different Dox levels (top panel). Dox was titrated up to 1000 ng/ml to exclude cell toxicity. Absence of KDM5B protein induction in WM3734[Tet3G] control cells (middle) and WM3734[Tet3G-EGFP] control cells (bottom). (**D**) Representative immunoblots of KDM5B and histone H3K4me3 after 22 days of Dox induction in WM3734[Tet3G-KDM5B] cells (n=2).
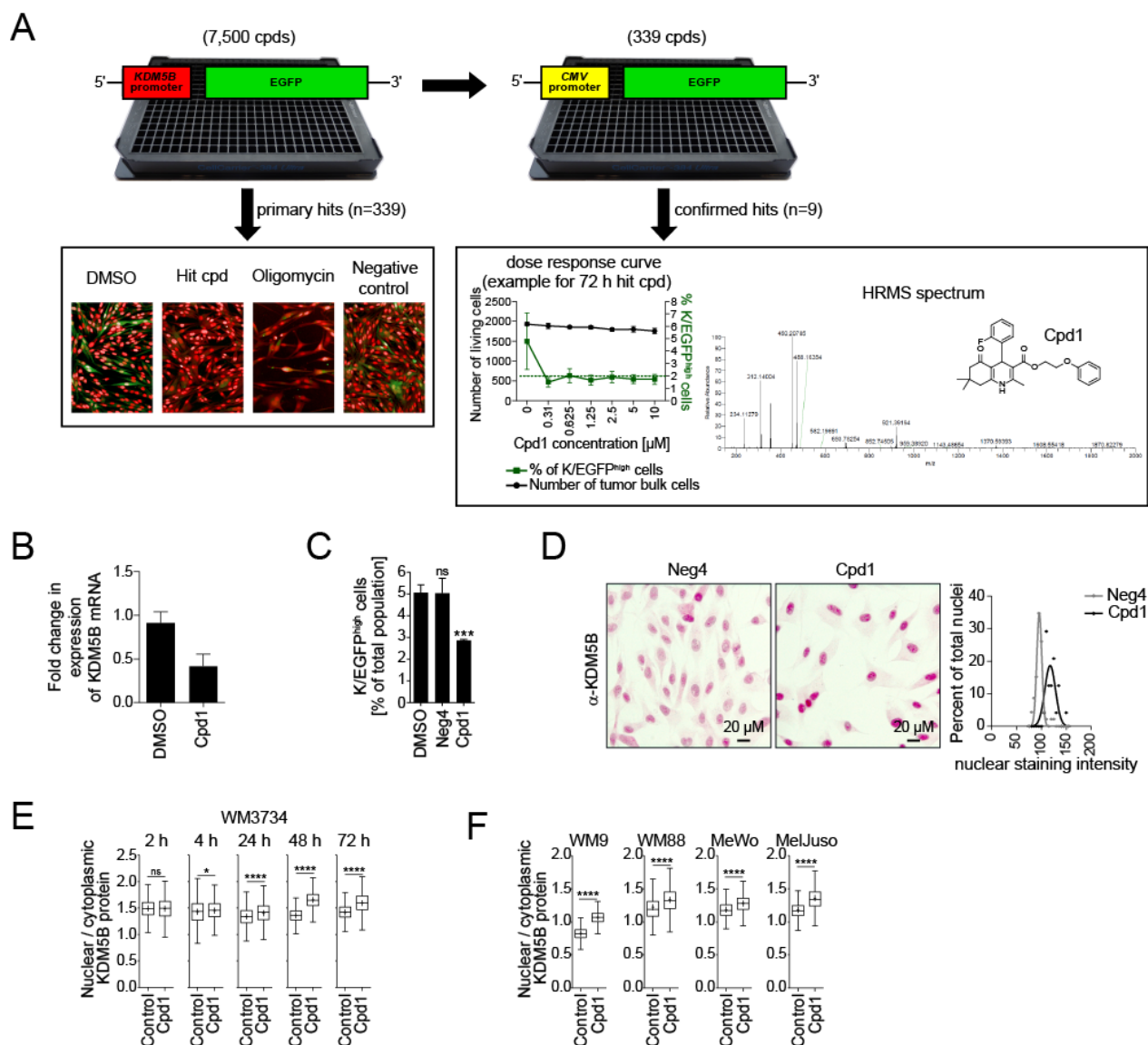
Figure S3

Figure S3. Screening for small chemical compounds that modulate KDM5B expression, Related to Figure 1. (**A**) Schematic of the phenotypic compound screening assay consisting of a primary screen based on the WM3734[KDM5Bprom-EGFP] cell model and a counter screen with WM3734[CMVprom-EGPF] control cells performed on an Opera High Content Screening system. Dose

response curves were done for confirmed hit compounds, as e.g. compound no. 1 (abbreviated Cpd1). The structural formula and HRMS purity analysis of Cpd1 is shown at the right. For more details, see methods. (**B**) Quantitative PCR detection of endogenous KDM5B mRNA transcripts (all isoforms covered) after 72 h of Cpd1 treatment in WM3734 cells. Shown is one representative experiment out of 4 independent replicates. (**C**) Independent hit validation by flow cytometric detection showed reduced KDM5B-promoter-driven EGFP (K/EGFP) expression in WM3734 cells after 72 h of treatment with the hit compound Cpd1 (10 μM) compared to DMSO and the structure homologue compound Neg4 (10 μM) which lacks comparable activity. Shown are summarized data (mean ±SD) of 3 independent experiments; significance was tested by t-test (***$P \leq 0.001$). (**D**) Anti-KDM5B nuclear immunostaining of WM3734 melanoma cells after 72 h of Cpd1 vs. Neg4 treatment (10 μM). Left, representative pictures; right, quantitation shown as normalised frequency distribution of nuclear staining intensity. (**E**) Digital microscopic quantitation of nuclear vs. cytoplasmic KDM5B protein expression in WM3734 cells after Cpd1 treatment over time and (**F**) across different melanoma cell lines (WM9, WM88, MeWo, MelJuso) after 72 h of treatment. Mean ±SD; *$P \leq 0.05$, ****$P \leq 0.0001$ by t-test. Box-and-whiskers represent median values and interquartile range; the mean values are plotted as crosses. Shown are results from 2-4 independent replicates with at least 3 quantified images per experiment.
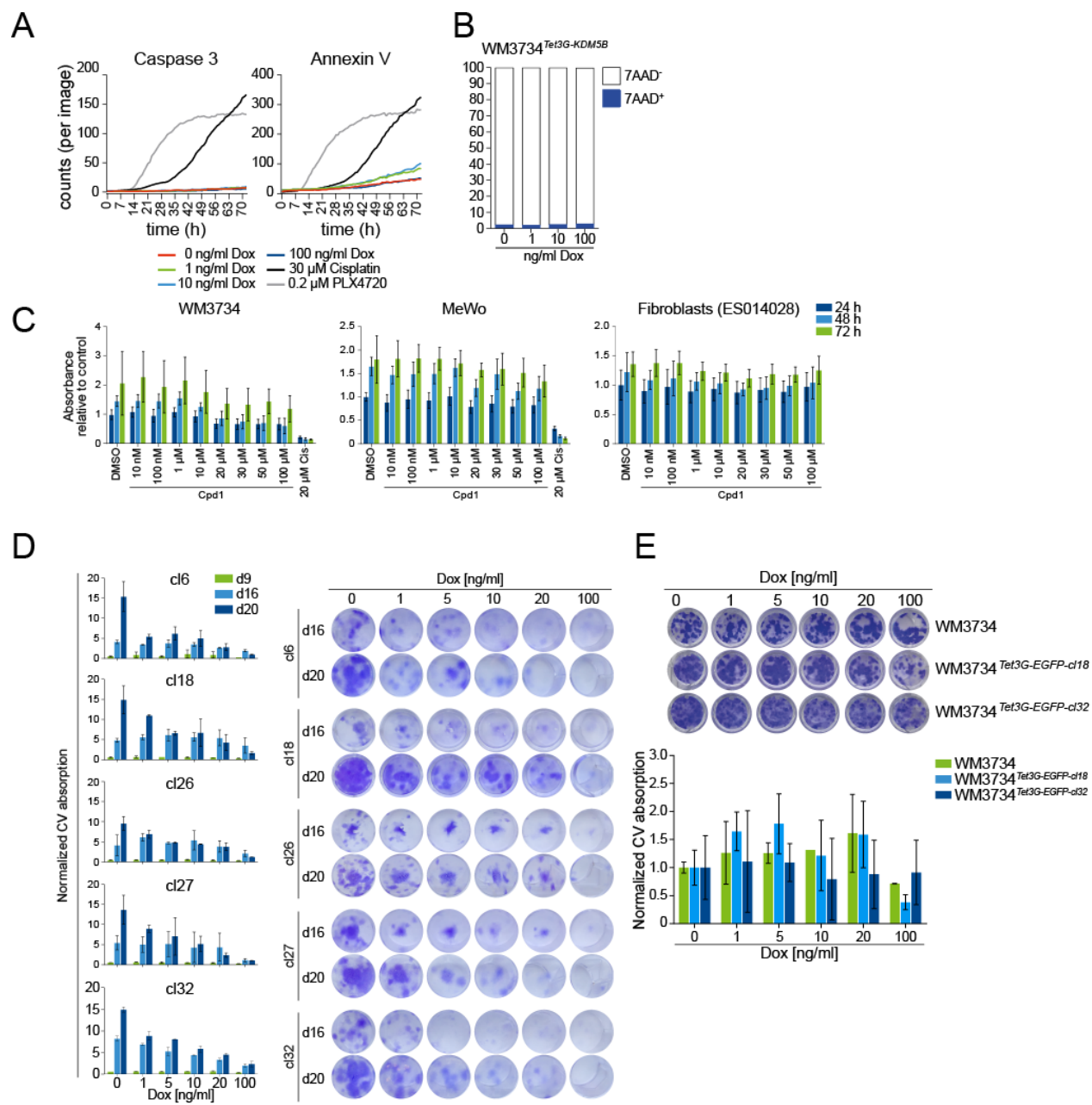
Figure S4

Figure S4. *In vitro* effects of up-scaled KDM5B expression, Related to Figure 2. (**A**) Caspase 3 and annexin V detection over 72 h determined by IncuCyte analysis. Cisplatin and PLX4720 were used as positive controls for induction of apoptosis. Shown is one representative experiment out of three independent biological replicates. (**B**) Flow cytometric determination of 7AAD$^+$ dead cells after 48 h of KDM5B induction by Dox. Shown is one representative experiment out of 4 independent replicates. (**C**) MTT assay after 24, 48, and 72 h of Cpd1 treatment in WM3734 and MeWo melanoma cells compared to primary ES014028 fibroblasts. Data are depicted as mean ±SD. Shown is one representative experiment out of three independent biological replicates. (**D**) Long-term clonogenic growth assay after gradual KDM5B induction over 9, 16, and 20 days with Dox from 5 different WM3734$^{Tet3G-KDM5B}$ clones (left, crystal violet quantitation; right, representative pictures from day 16 and 20). Data are shown as mean ±SD. (**E**) Clonogenic long-term growth of WM3734$^{Tet3G-EGFP}$ control clones and naïve WM3734 cells after 20 days of Dox exposure (upper panel, representative pictures; lower panel, crystal violet quantitation). Data are shown as mean ±SD.
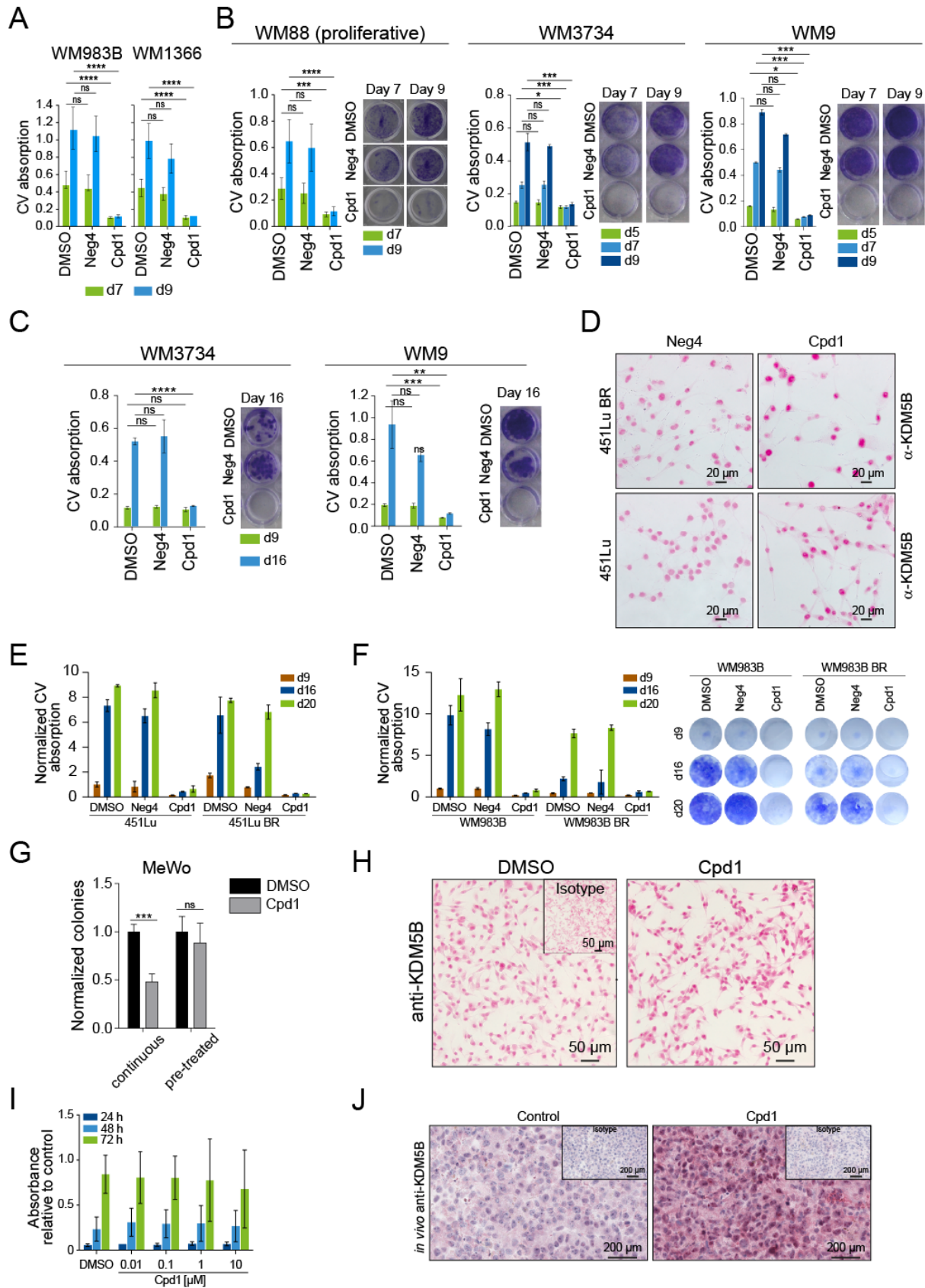
Figure S5

9

Figure S5. *In vitro* and *in vivo* effects of up-scaled KDM5B expression, Related to Figure 2.

(**A**) Quantitation of clonogenic growth assay of Fig. 2E. Shown is one representative experiment out of 3 independent biological replicates (mean ±SD). Significance was assessed by t-test (****P≤0.0001). (**B**) Clonogenic growth assay of WM88, WM3734 and WM9 cells continuously treated over 5, 7 and 9 days with 10 µM of Cpd1 or Neg4 (left, crystal violet quantitation; right representative pictures from day 7 and 9). Shown is one representative experiment out of 3 independent biological replicates (mean ±SD). Significance was assessed by t-test (*P≤0.05, ***P<0.001, ****P≤0.0001). (**C**) Clonogenic growth assay of WM3734 and WM9 cells continuously treated over 9-16 days with 10 µM of Cpd1 or Neg4 (left, crystal violet quantitation (mean ±SD); right representative images from day 16). Significance was determined by t-test (**P≤0.01, ***P<0.001, ****P≤0.0001). (**D**) Representative images of anti-KDM5B immunostaining of chronically PLX4720-resistant 451Lu BR vs. treatment-naïve 451Lu melanoma cells. Cells were treated for 72 h with Cpd1 (10 µM) or Neg4 (10 µM). (**E**) Quantitation of clonogenic growth assay of 451Lu and 451Lu BR cells shown in Fig. 2F. Data are depicted as mean ±SD. (**F**) Clonogenic growth assay of WM983B and PLX4720-resistant WM983B-BR cells treated over 9,16 and 20 days with 10 µM of Cpd1 or Neg4 (left, crystal violet quantitation; right, representative pictures). Data are depicted as mean ±SD. (**G**) Soft agar colony formation of MeWo cells under constant Cpd1 treatment or after pre-treatment with Cpd1 for 72 h before seeding. Shown are results of 2 independent experiments with each being performed in triplicate reaction. Data are shown as mean ±SD; ***P≤0.001 by t-test. (**H**) Anti-KDM5B nuclear immunostaining of CM melanoma cells after 72 h of in vitro Cpd1 or as control DMSO treatment. (**I**) MTT assay after 24, 48, and 72 h of Cpd1 treatment in CM cells (mean ±SD, n=3). (**J**) Anti-KDM5B nuclear immunostaining of CM melanoma tumor grafts from Cpd1-treated mice and control mice.
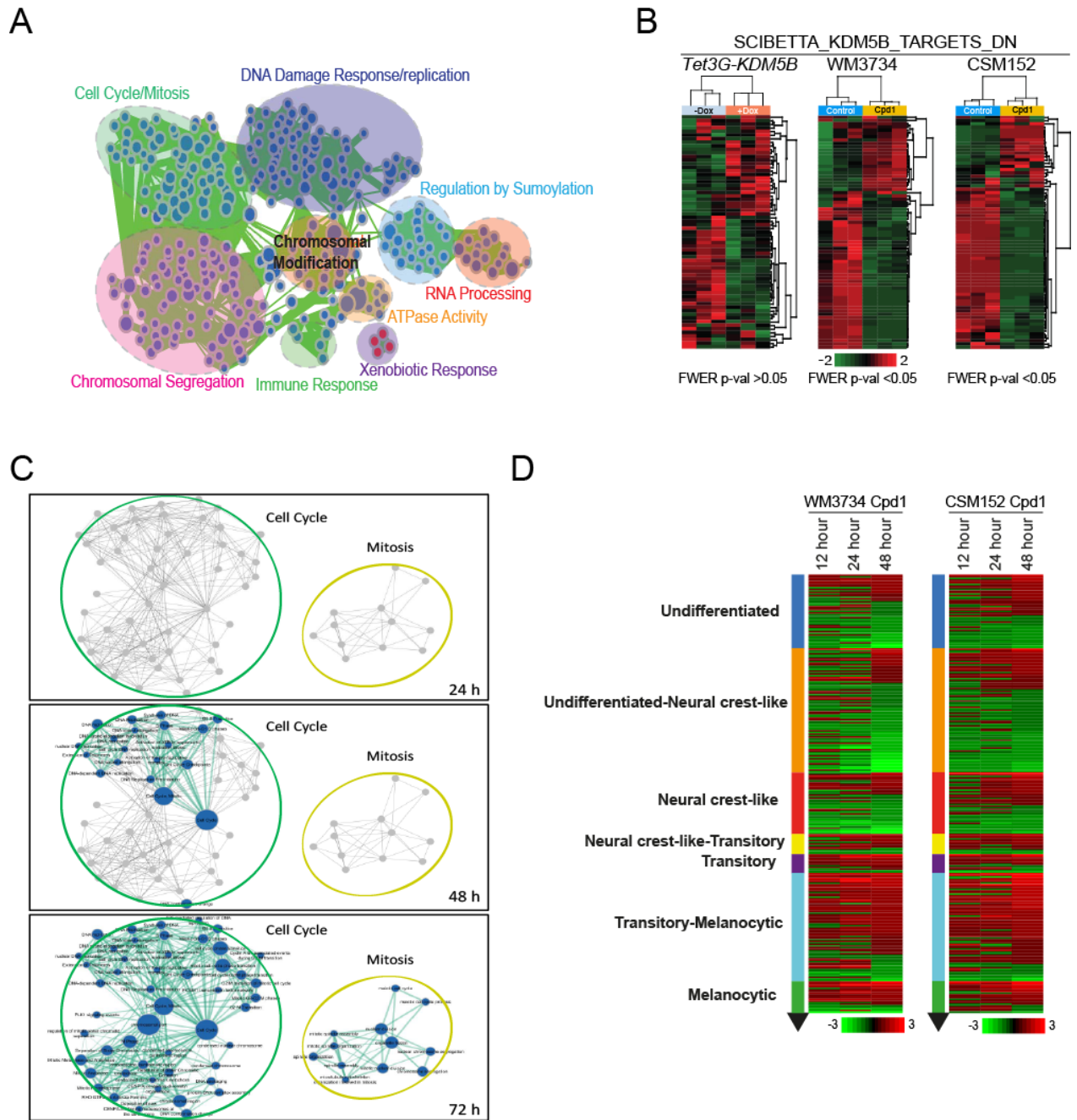
Figure S6

Figure S6. Transcriptional shifts as a result of up-scaled KDM5B expression, Related to Figure 3. (**A**) Overview of KDM5B-dependent regulatory pathways. Cytoscape enrichment analysis of significantly regulated gene signatures detected in RNAseq in WM3734 and patient-derived, short-term cultured CSM152 cells treated with Cpd1 over 72 h. Red node, enrichment in

treatment group; blue node, decrease. The size of the nodes represents the number of genes included. (**B**) Heatmaps of the SCIBETTA_KDM5B_TARGETS_DN (DN='down') motif [1] from WM3734*Tet3G-KDM5B* cells after 72 h of Dox treatment compared to corresponding WM3734 cells and short-term cultured CSM152 cells after 72 h of Cpd1 treatment (red, upregulated; green downregulated genes). Significance is indicated by FWER p-val < 0.05. (**C**) Enrichment analysis of cell cycle- and mitosis-controlling transcripts detected in WM3734*Tet3G-KDM5B* cells after 24, 48 and 72 h of Dox treatment. GSEA visualizations for each time point were combined in Cytoscape. Blue nodes represent enrichment in the control group; grey nodes were not yet present at the respective time point, the size of the nodes reflects the number of genes included. (**D**) Heatmap of Tsoi differentiation signature [2] from WM3734 and CSM152 cells after 12 h, 24 h and 48 h Cpd1 treatment ranked by expression at 48 h (red, upregulated; green downregulated genes).

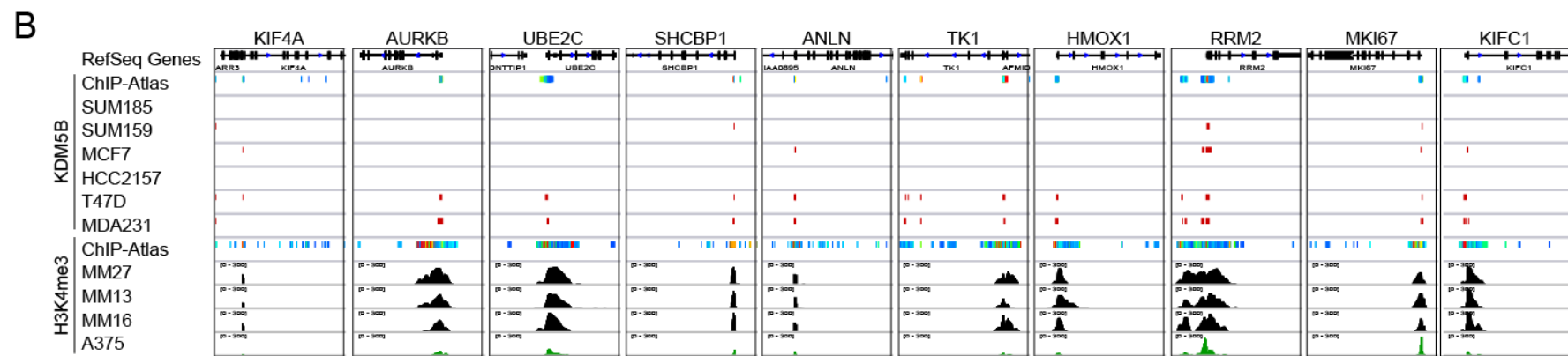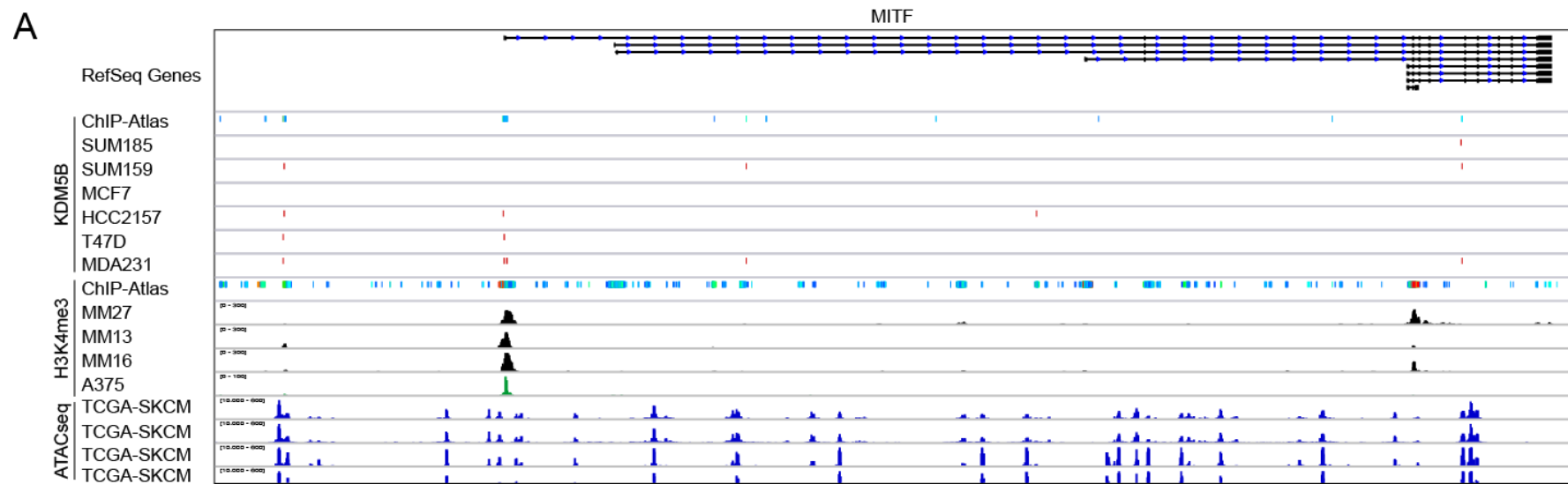Figure S7

Figure S7. Potential KDM5B binding sites at the MITF, cytokinesis, and mitotic spindle assembly genes, Related to Figure 3. (**A**) *In silico* analysis of the MITF gene based on publicly available KDM5B- and H3K4me3-ChIPseq data from breast cancer cell lines SUM185, SUM159, MCF7, HCC2157, T47D, and MDA231 (GSE46073 [3]), melanoma cell lines MM27, MM13, MM16 (GSE71854 [4]) and A375 (GSE99835 [5]), ChIP-Atlas [6] and ATACseq data from skin cancers of TCGA [7]. (**B**) *In silico* analysis of cytokinesis genes or mitotic spindle assembly of publicly available KDM5B- and H3K4me3-ChIPseq data from breast cancer cell lines SUM185, SUM159, MCF7, HCC2157, T47D, and MDA231 (GSE46073 [3]) and melanoma cell lines MM27, MM13, MM16 (GSE71854 [4]) and A375 (GSE99835 [5]) and ChIP-Atlas [6].
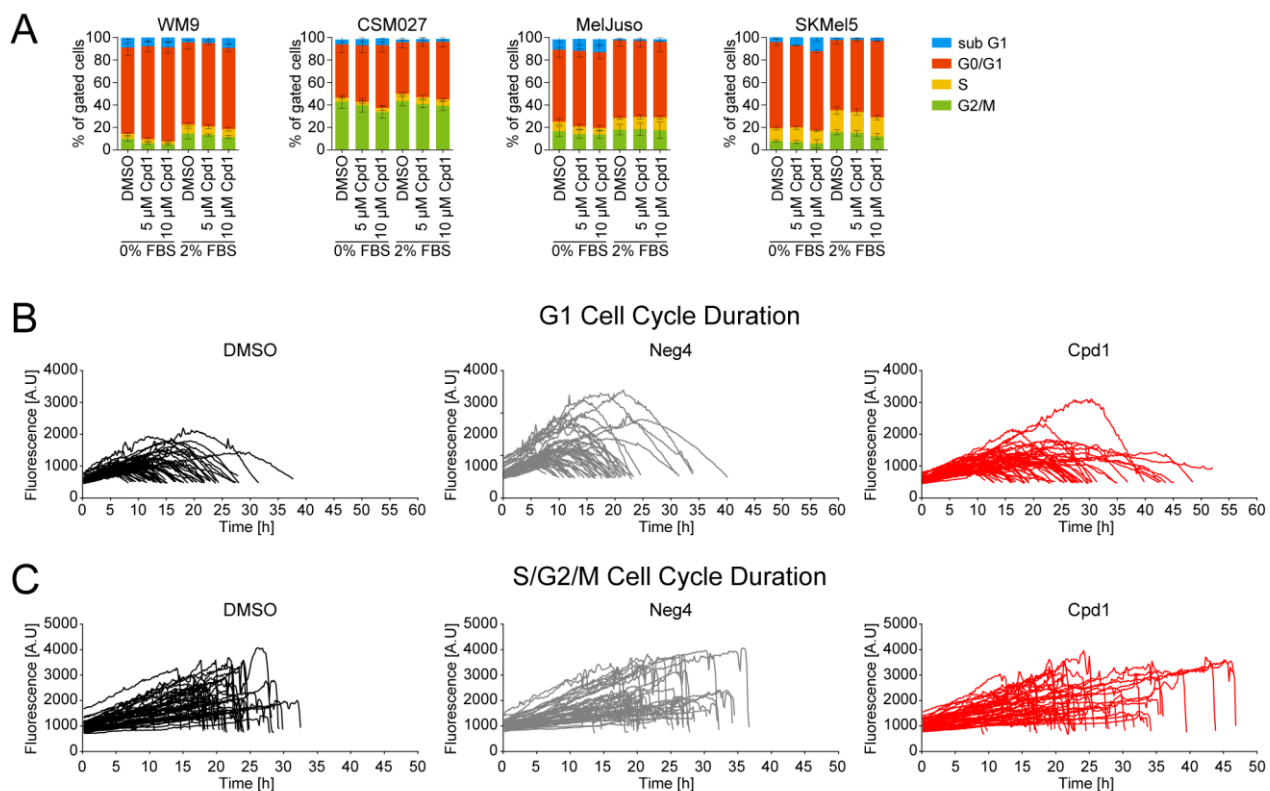
Figure S8. Effects of up-scaled KDM5B expression on cell cycle, Related to Figure 4. (**A**) Propidium iodide flow cytometric cell cycle analysis after 72 h of Cpd1. WM9, CSM027, MelJuso, and SKMel5 cells were either continuously starved (0% FBS) or starved and then released by 2% FBS. Shown are results from 4 independent experiments. Mean ±SD. (**B** and **C**) G1 (**B**) and S/G2/M (**C**) cell cycle duration of single cells (n=49) measured by FUCCI time-lapse imaging after 72 h of treatment with Cpd1 (10 µM) vs. DMSO or Neg4 (10 µM) controls.
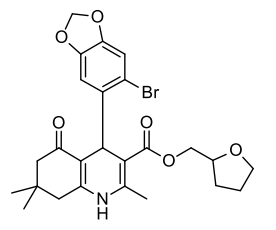
Figure S9

Figure S9. **Marker confirmation in endogenous KDM5B^{high} melanoma cells, Related to Figure 4.** WM3734[KDM5Bprom-EGFP] cells w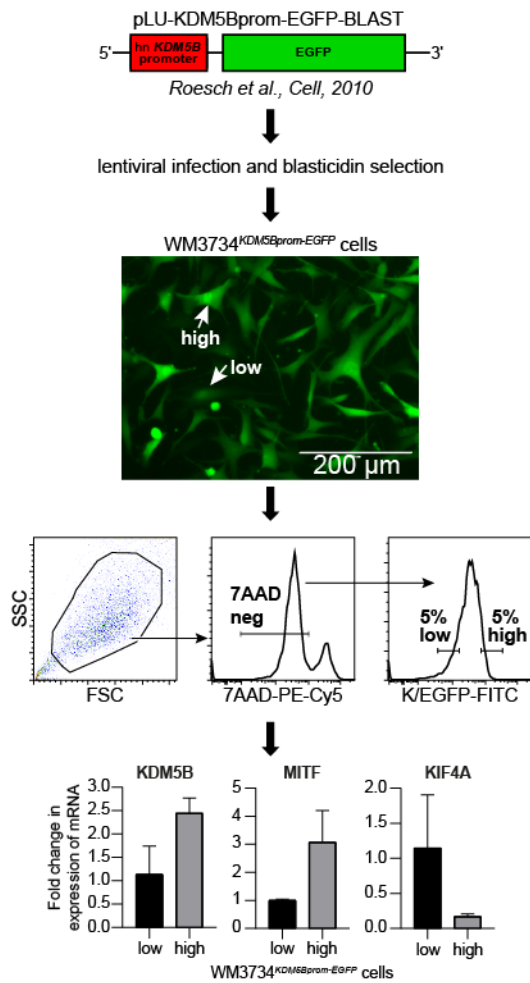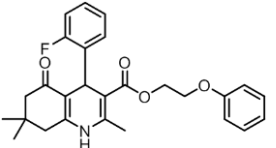ere separated into KDM5B^{high} and KDM5B^{low} populations according to their K/EGFP signal intensity. The thresholds for sorting were set to the highest/lowest 5% of K/EGFP signal intensity. mRNA of KDM5B^{high} vs. KDM5B^{low} cells was tested by qPCR for the indicated genes. Mean ±SD.

Table S1. Screening assay results for the selected hit (Cpd1) and control (Neg4) compound. Related to Figure S3.

Cmpd Identifier	Structure	Mother plate (WellIndex)	PS % of K/EGFP^{high} cells mean	HC run I % of K/EGFP^{high} cells mean ±SD (n=3)	HC run II % of K/EGFP^{high} mean ±SD (n=2)	HC run III % of K/EGFP^{high} cells mean ±SD (n=3)	Mean
27849_ChemDiv _2191-2790 **(Cpd1)**		CBN_000012_D01 (Well I07)	**2.00**	0.95 ± 0.37	1.18 ± 0.24	2.27 ± 0.15	**1.47**
26798_ChemDiv _2732-4408 **(Neg4)**		CBN_000009_D01 (Well N7)	**3.85**	no Hit (n.a.)	no Hit (n.a.)	no Hit (n.a.)	

PS = primary Screen
HC = Hit Confirmation

Table S2. Significantly regulated genes detected by RNAseq of cells treated with Cpd1 (WM3734 and CSM152 cells, 10 µM Cpd 1for 72 h,) or doxycycline (WM3734$^{Tet3G\text{-}KDM5B}$ **cells, 10 ng/ml for 24 h, 48 h or 72 h**). Related to Figure 3 and S6.

Please see separately uploaded Table.

Table S3. Normalized enrichment scores (NES) and false discovery rate (FDR) for the heatmaps of the 'Tsoi et. al differentiation signature'[2] shown in Figure 3C and S6D. Related to Figure 3 and S6.

NES	10 dox vs 0 dox (24 h)			WM3734 Cpd1 vs DMSO			CSM152 Cpd1 vs DMSO		
Signature	24 h	48 h	72 h	12 h	24 h	48 h	12 h	24 h	48 h
Undifferentiated	2.13	-1.52	-1.50	-1.38	-1.35	-1.93	-1.58	-1.14	-1.76
Undifferentiated-neural crest-like	1.27	-2.83	-2.69	-1.93	-1.86	-2.08	-2.15	-1.51	-1.74
Neural crest-like	-1.73	-2.67	-2.60	-2.26	-1.93	-1.79	-1.17	-1.64	-1.27
Neural crest-like-transitory	-1.59	1.24	1.30	-1.18	1.30	-1.42	1.15	1.31	1.17
Transitory	0.87	2.17	2.16	-1.04	1.02	-0.89	1.13	1.89	1.66
Transitory-melanocytic	-1.42	2.66	2.90	1.47	1.66	1.61	1.52	2.07	1.67
Melanocytic	0.80	1.96	2.30	-1.53	1.02	1.07	1.31	1.55	1.79

FDR	10 dox vs 0 dox(24 h)			WM3734 Cpd1 vs DMSO			CSM152 Cpd1 vs DMSO		
Signature	24 h	48 h	72 h	12 h	24 h	48 h	12 h	24 h	48 h
Undifferentiated	0.00	0.03	0.03	0.11	0.09	0.00	0.03	0.28	0.03
Undifferentiated-neural crest-like	0.25	0.00	0.00	0.01	0.00	0.00	0.00	0.04	0.02
Neural crest-like	0.02	0.00	0.00	0.00	0.00	0.01	0.24	0.03	0.14
Neural crest-like-transitory	0.04	0.16	0.12	0.25	0.27	0.07	0.32	0.11	0.24
Transitory	0.93	0.00	0.00	0.39	0.55	0.64	0.26	0.00	0.01
Transitory-melanocytic	0.06	0.00	0.00	0.05	0.06	0.02	0.10	0.00	0.01
Melanocytic	0.79	0.00	0.00	0.06	0.42	0.35	0.22	0.04	0.00

Table S4. Significantly regulated genes detected by RNAseq of cells treated with Cpd1 (WM3734 and CSM152 cells, 10 μM for 12 h, 24 h and 48 h). Related to Figure S6.

Please see separately uploaded Table.

Table S5. Significantly regulated genes detected by mass spectrometry of WM3734 cells treated with 10 μM Cpd1 for 72 h. Related to Figure 4.

Please see separately uploaded Table.

Table S6. Primer Sequences. Related to Figure 1, 3, 4, S3 and S9.

Name	Species	Sequence (5'-3')	Source
AURKB fwd	human	CATCACACAACGAGACCTATCGCC	
AURKB rev	human	GGGTTATGCCTGAGCAGTTTGGAG	
KDM5B all isoforms fwd	human	AACAACATGCCAGTGATGGA	[8]
KDM5B all isoforms rev	human	TACCAGGTTTTTGGCTCACC	[8]
KDM5B transcript variant 1 fwd	human	AACCTCCGCCTCCTAGATTC	
KDM5B transcript variant 1 rev	human	CGTTGTCTCCTCGGGTTCTA	
KIF4A fwd	human	GAAGAAAACCAAGGCTGAAGGGG	
KIF4A rev	human	TGGAATCTCTGTAGGGCACAAAGC	
MITF fwd	human	CCGTCTCTCACTGGATTGGT	[9]
MITF rev	human	TACTTGGTGGGGTTTTCGAG	[9]
SHCBP1 fwd	human	TGTTTGACCAGACAGCCCTTGC	
SHCBP1 rev	human	TCATCCTCCTCTTCTTCATCCCAAC	
UBE2C fwd	human	GCATCAGAACCAGCTCAACA	
UBE2C rev	human	GGTTCTGGCATTTGGAGAAA	

18S fwd	human	CGCCGCTAGAGGTGAAATTC	
18S rev	human	TCTTGGCAAATGCTTTCGC	
Myco-SE	human	GGGAGCAAACAGGATTAGATACCC	10
Myco-AS	human	TGCACCATGTGTCACTCTGTTAACCTC	10
DCT fwd	murine	CAGCACAAGCGTGGAACAC, ID 28076935a1	11
DCT rev	murine	TGCGATCTGAGAAATCAAGCC, ID 28076935a1	11
MITF fwd	murine	CAAATGGCAAATACGTTACCCG, ID 8917552a1	11
MITF rev	murine	CTCCCTTTTTATGTTGGGAAGGT, ID 8917552a1	11
MLANA fwd	murine	CTGCTGGTACTGTAGAAGACGA, ID 110625784c2	11
MLANA rev	murine	GGCTCTCACATGAGCATCTTTC, ID 110625784c2	11
TYR fwd	murine	ATAGGTGCATTGGCTTCTGG	12
TYR rev	murine	TCTTCACCATGCTTTTGTGG	12
18S fwd	murine	GGGCGGAGATATGCTCATGTG	
18S rev	murine	TCTGGGATCTTGTACTGTCGT	

Supplemental movies. Live cell imaging of WM3734 cells treated with DMSO, Neg4 (10 µM) or Cpd1 (10 µM) over 5 days. Related to Figure 4.

Please see separately uploaded supplementary material.

References

1   Scibetta, A. G. *et al.* Functional analysis of the transcription repressor PLU-1/JARID1B. *Mol Cell Biol* **27**, 7220-7235 (2007).
2   Tsoi, J. *et al.* Multi-stage Differentiation Defines Melanoma Subtypes with Differential Vulnerability to Drug-Induced Iron-Dependent Oxidative Stress. *Cancer Cell* **33**, 890-904.e895, doi:10.1016/j.ccell.2018.03.017 (2018).
3   Yamamoto, S. *et al.* JARID1B is a luminal lineage-driving oncogene in breast cancer. *Cancer Cell* **25**, 762-777, doi:10.1016/j.ccr.2014.04.024 (2014).

4   Bossi, D. *et al.* In Vivo Genetic Screens of Patient-Derived Tumors Revealed Unexpected Frailty of the Transformed Phenotype. *Cancer Discov* **6**, 650-663, doi:10.1158/2159-8290.CD-15-1200 (2016).

5   Joung, J. *et al.* Genome-scale activation screen identifies a lncRNA locus regulating a gene neighbourhood. *Nature* **548**, 343-346, doi:10.1038/nature23451 (2017).

6   Oki, S. *et al.* ChIP-Atlas: a data-mining suite powered by full integration of public ChIP-seq data. *EMBO Rep* **19**, doi:10.15252/embr.201846255 (2018).

7   Corces, M. R. *et al.* The chromatin accessibility landscape of primary human cancers. *Science (New York, N.Y.)* **362**, doi:10.1126/science.aav1898 (2018).

8   Roesch, A. *et al.* A temporarily distinct subpopulation of slow-cycling melanoma cells is required for continuous tumor growth. *Cell* **141**, 583-594 (2010).

9   Smith, M. P. *et al.* A PAX3/BRN2 rheostat controls the dynamics of BRAF mediated MITF regulation in MITF(high) /AXL(low) melanoma. *Pigment Cell Melanoma Res* **32**, 280-291, doi:10.1111/pcmr.12741 (2019).

10   Ossewaarde, J. M., de Vries, A., Bestebroer, T. & Angulo, A. F. Application of a Mycoplasma group-specific PCR for monitoring decontamination of Mycoplasma-infected Chlamydia sp. strains. *Appl Environ Microbiol* **62**, 328-331 (1996).

11   Spandidos, A., Wang, X., Wang, H. & Seed, B. PrimerBank: a resource of human and mouse PCR primer pairs for gene expression detection and quantification. *Nucleic Acids Res* **38**, D792-799, doi:10.1093/nar/gkp1005 (2010).

12   Riesenberg, S. *et al.* MITF and c-Jun antagonism interconnects melanoma dedifferentiation with pro-inflammatory cytokine responsiveness and myeloid cell recruitment. *Nat Commun* **6**, 8755, doi:10.1038/ncomms9755 (2015).